NACA

RESEARCH MEMORANDUM

EXPERIMENTAL HEAT-TRANSFER AND FRICTION COEFFICIENTS

FOR AIR FLOWING THROUGH STACKS

OF PARALLEL FLAT PLATES

By Eldon W. Sams and Walter F. Weiland, Jr.

Lewis Flight Propulsion Laboratory
Cleveland, Ohio

NATIONAL ADVISORY COMMITTEE
FOR AERONAUTICS
WASHINGTON
August 19, 1954

129617091   3501501

NATIONAL ADVISORY COMMITTEE FOR AERONAUTICS

RESEARCH MEMORANDUM

EXPERIMENTAL HEAT-TRANSFER AND FRICTION COEFFICIENTS

FOR AIR FLOWING THROUGH STACKS

OF PARALLEL FLAT PLATES

By Eldon W. Sams and Walter F. Weiland, Jr.

SUMMARY

An investigation is being conducted at the NACA Lewis laboratory to obtain forced-convection heat-transfer and pressure-drop data for flow of air between electrically heated parallel flat plates stacked to form passages of short length-to-effective-diameter ratio. Two such stacks of plates were alined in series in the direction of air flow, with a 1/4-inch spacing between plates in each stack. Data were obtained for three gap spacings between stacks of 1/32, 1/8, and 1/4 inch, as well as for various degrees of plate misalinement between stacks, and also with the upstream stack removed from the tunnel. The primary purpose of the investigation is to determine the interference effects of the upstream stack of plates on the heat-transfer and friction characteristics of the downstream stack.

Data were obtained over a range of Reynolds number from 15,000 to 80,000, average surface temperatures from 661° to 683° R, heat fluxes up to 8080 Btu per hour per square foot, inlet air temperature of about 518° R, and inlet pressures up to 45 inches of mercury absolute, and with heat addition to the downstream stack only.

The average and local heat-transfer coefficients obtained for the downstream stack with the two stacks alined were slightly higher than the values predicted from established data on round tubes for the length-diameter ratio used herein. Also, the effects of changes in plate misalinement and gap spacing between stacks were found to be negligible. The friction factors for the upstream stack, when fully corrected for nonfriction losses and length-diameter ratio effects, were in good agreement with data for smooth round tubes; for the downstream stack, the friction factors were lower than those for smooth tubes when a uniform velocity profile at the entrance was assumed, and higher than those for smooth tubes when a fully developed velocity profile at the entrance was assumed in the correction of the data for entrance effects.

INTRODUCTION

The present investigation was undertaken to obtain forced-convection heat-transfer and pressure-drop data for flow of air between electrically heated parallel flat plates forming passages of short length-to-effective-diameter ratio. More specifically, the program was designed to provide these data for successive stacks of plates wherein the effects of such configuration variables as distance between parallel plates, gap spacing between successive stacks, and degree of misalinement between plates in successive stacks are to be evaluated for a range of Reynolds numbers, plate surface temperatures, and heat fluxes.

These data are of interest in the design of heat exchangers of similar geometries (and plain or interrupted surfaces), where advantage can be taken of the increased heat transfer associated with flow in passages of short length-diameter ratio. In addition to average heat-transfer values, the design of heat exchangers may require a more detailed knowledge of local surface-temperature gradients or limiting local temperatures, in which case recourse must be made to local heat-transfer values. Both local and average heat-transfer coefficients are reported herein.

In the present investigation, heat-transfer and pressure-drop data were obtained for two stacks of parallel flat plates with a 1/4-inch spacing between plates in each stack, various degrees of plate misalinement, and various gap spacings (1/32, 1/8, and 1/4 in.) between stacks, as well as with the upstream stack removed. The data reported herein were obtained with heat addition to the downstream stack only. Data were obtained over a range of Reynolds numbers from 15,000 to 80,000, average surface temperatures from 661° to 683° R, heat fluxes up to 8080 Btu per hour per square foot, an inlet air temperature of about 518° R, and inlet pressures up to 45 inches of mercury absolute.

The results are presented herein in the form of curves of average values of a Nusselt-Prandtl number relation ($Nu/Pr^{0.4}$) against Reynolds number, of local heat-transfer coefficients and plate temperatures against distance from leading edge of plate, and of average friction factors against Reynolds number.

APPARATUS

Air and Electrical Systems

A schematic diagram of the test section and related components of the air and electrical systems used in this investigation is shown in figure 1.

Air system. - As indicated in figure 1, air at 110 pounds per square inch gage passed through a pressure-regulating valve, a filter, and an orifice run consisting of an air straightener and an A.S.M.E. type flat-plate orifice where the air flow was measured before entering the test section. The air then passed through the test section which consisted of an approach section, the two stacks of electrically heated flat plates, and a three-pass mixing tank having a thermally insulated approach, after which the air discharged to the atmosphere. A window and light source were provided upstream of the test section for visual observation of the flat plates during testing.

The temperature of the air entering the test section was measured by an iron-constantan thermocouple upstream of the approach section; the temperature of the air leaving the test section was similarly measured by two thermocouples just downstream of the mixing screens in the mixing tank.

Electrical system. - Provisions were made for electrically heating both stacks of flat plates, although only the downstream stack was heated for the data reported herein, the electrical system for each stack being separate and independently controlled (see fig. 1). Electric power was supplied to each stack through a variable transformer and a power transformer, the latter being connected by flexible cables to bus bars which were fastened to the two outer plates (top and bottom) of each stack; the plates in each stack were connected in series. The capacity of the electrical equipment for each stack was 12 kilovolt-amperes at a maximum of 12 volts across the stack.

Test Section

Installation. - A schematic diagram of the test section is shown in figure 2(a). The two stacks of flat plates were independently mounted in a steel tunnel provided with micrometer screws to permit vertical movement of the stacks for plate alinement and misalinement between stacks. The two stacks could be separated by 1/32-, 1/8-, or 1/4-inch-thick transite spacers having a 2- by 3-inch opening in the center. Similar spacers of 3/4-inch thickness were provided before the upstream stack and after the downstream stack, with a high-temperature rubber gasket recessed into the spacer to provide an air seal between stack and spacer. Transite plates (not shown) running the length of both stacks were provided between the stack and tunnel side walls with sufficient clearance to allow vertical movement of the stacks; these transite plates were grooved vertically to allow plate instrumentation leads to be brought up the side of the stack. A wooden approach section (24 in. long with 2- by 3-in. opening) having a rounded entrance was located before the upstream stack. A three-pass mixing tank was located after the downstream stack; the mixing-tank approach section was thermally

insulated and contacted a rubber gasket in the rear spacer. Two screens were provided in the mixing tank center passage for thorough mixing of air ahead of the exit air thermocouples.

The two stacks of plates tested were identical, one such stack being shown in more detail in figure 2(b). The stack consisted of nine flat plates stacked vertically with a 0.25-inch spacing between plates. This spacing was provided by either one 1/4-inch or two 1/8-inch spacer strips running the length of the plates along either side. The strips (conductors or insulators) were stacked in such a manner as to provide an electrical series connection between plates. An insulator plate and a steel support plate were provided over the two outside plates in the stack (fig. 2(a)), the entire stack being clamped together by four insulated bolts through the stack. The bus bars supplying electrical power to the plates were silver-soldered to the conductor strips of the two outside plates in the stack. Bosses which were provided on the bottom support plate of the stack rested on micrometer screws fastened to the bottom tunnel wall, thereby providing means for vertical movement to obtain alinement or misalinement of the two stacks.

Instrumentation. - The instrumentation for each stack of plates is indicated in figure 2(b). The flat plates were 0.018 inch thick, 3 inches wide (exposed to flow), and 3.5 inches long. Iron-constantan thermocouples were imbedded in the plates by cutting grooves 0.014 inch wide and 0.008 inch deep into the plate at right angles to the direction of flow. The iron-constantan wires (0.005-in. diameter including insulation) were then laid in the groove and covered with an insulating cement. The thermocouple leads from the edge of the plate were secured to the outer edge of the spacer strips (between plates) and then brought up the sides of the stack. Thermocouples were placed in the various plates of the stack at the locations indicated in figure 2(c). The number of thermocouples was progressively decreased toward the outer plates, giving a total of 68 thermocouples in each stack.

Voltage-drop leads were also silver-soldered to the conductor strips at the edges of each plate (the conductor strips being spot welded to the individual plates) in such a manner as to obtain the voltage drop across each plate. Over-all voltage-drop readings were also obtained for the stack.

Static-pressure taps were located in each of the three transite spacers as indicated in figure 2(a), the static taps being placed at the center of the bottom and side surfaces of the opening in each case. The various pairs of static taps across each stack were read separately on U-tube water manometers to obtain the pressure drop across each stack.

A photograph of the complete test section is shown in figure 3. All thermocouple and voltage drop leads were brought out between two rubber gaskets under an access plate on top of the tunnel. The access plate covered both stacks of heated plates; it also provided seals for the bus bars leaving the tunnel and fittings for insertion of probes into the spacer openings.

METHOD OF CALCULATION

Evaluation of average plate and stack temperature. - As previously indicated in figure 2(c), thermocouples were located down the center line of the plate at various distances from the plate leading edge with a similar row of thermocouples along a line 3/4 inch from the center line toward either side of the plate. The plate temperature gradients normal to the direction of air flow were found to be small compared to gradients in the flow direction; therefore, the temperature gradient for the plate can be well represented by plotting the plate center line temperature against distance from the leading edge. The gradients for each plate in the stack were plotted in this manner; where center line thermocouples were not available (see fig. 2(c)), the average of the two side row thermocouples was used. The average temperature for each plate was then obtained by dividing the measured area under the curve of the plate center line temperature against distance from leading edge by the plate length. The average surface temperature for the entire stack was then taken as the arithmetic average of the various average plate temperatures weighted according to the surface area exposed to flow. (The two outside plates were exposed to flow on one side only.)

Average heat-transfer coefficients. - The average heat-transfer co-efficient for the stack was computed from the relation (symbols are defined in appendix A):

$$h_{av,st} = \frac{(Q/S)_{av,st}}{(T_s - T_b)_{av,st}} = \frac{Wc_p(T_4 - T_1)_{st}/S_{st}}{(T_s - T_b)_{av,st}} \tag{1}$$

The average bulk temperature $T_{b,av}$ was taken as the arithmetic average of the inlet-air and exit-air total temperatures, T_1 and T_4, respectively. The heat-transfer surface area S was taken as the total surface area of the plates exposed to flow. The exposed surface area contributed by the spacer strips between plates is not included, but would have a negligible effect on h. The values for physical properties of air used herein are presented in figure 4.

Local heat-transfer coefficients. - Local heat-transfer coeffi-
cients for the center plate (plate 5) in the stack were evaluated in
the following manner. The local heat-transfer coefficient at any dis-
tance from the leading edge was taken as

$$h_l = \frac{(Q/S)_l}{(T_s - T_b)_l} = \frac{(Q/S)_{av} \; P_l/P_{av}}{(T_s - T_b)_l} \tag{2}$$

where all terms in the equation apply to the number 5 plate only.
For the number 5 plate, $(Q/S)_{av}$ was obtained by the relation

$$(Q/S)_{av,P} = (Q/S)_{av,st} \; E_P/E_{st} \tag{3}$$

$T_{b,l}$ was assumed to vary linearly with X (distance from plate leading
edge) between T_1 and T_4; $T_{s,l}$ was obtained from the plot of local
plate temperature against X as explained in the previous section.
This curve was also used to evaluate P_l/P_{av} in equation (2) in the
following manner: Inasmuch as the voltage drop across the plate is es-
sentially constant at any distance from leading edge X, and since heat
conduction along the plate can be neglected, the local power generation
at any point X is given by

$$P_l = E_P{}^2/R_l' = C/r_l \tag{4}$$

That is, the local power generation at any point (distance X from
leading edge) in the plate is inversely proportional to the electrical
resistivity r at the point; hence from a curve of electrical resis-
tivity r against temperature for the plate material and the curve of
$T_{s,l}$ against X, a curve of $1/r_l$ against X was plotted for the
plate. By graphically integrating this curve to obtain $1/r_{av}$, the
ratio of $1/r_l$ to $1/r_{av}$ (which also represents P_l/P_{av}) was then
plotted against distance from leading edge X. The local heat-transfer
coefficients h_l for the number 5 plate could then be computed from
equation (2) and plotted against X.

Average friction coefficients. - The method used for computing the
average friction coefficients for the individual stacks is as follows:
The friction coefficients are based on measured static-pressure drops
which were corrected for entrance, exit, vena contracta, and momentum
losses. The equations used in calculating these losses are derived in
appendix B. The values of measured pressure drop, as previously ex-
plained, were obtained from several pairs of static taps located in the
transite spacers on either side of and between the stacks (fig. 2(a)).
The pressure drop across the upstream stack was taken as the average of
the pressure drops measured by the taps in the two sides of the spacer

opening. Because of slight surface interruptions between stacks, static
probes were used in measuring the drop across the downstream stack. The
equations derived in appendix B result in the following evaluation of
friction factor: The fully corrected average half-friction factor is
defined as

$$(f/2)_{corr} = \frac{\Delta p_{corr}}{8 \, \frac{L}{D_e} \, \frac{G^2}{2g\rho_{av}}} \tag{5}$$

where ρ_{av} was evaluated with the total temperature and the static
pressure in the center window opening (negligible error for range of
conditions investigated); and

$$\Delta p_{corr} = \left[\Delta p_{meas} - \left(\Delta p_{en} + \Delta p_{ex} + \Delta p_{mom} + \Delta p_{vc} \right) \right] \tag{6}$$

where:

$$\Delta p_{en} = \frac{G_2^2}{2g\rho_1} \left(1 - F^2 \right) \tag{7}$$

$$\Delta p_{ex} = \frac{G_1^2}{g\rho_1} \frac{1 + \beta}{1 - \alpha} \left(1 - \frac{1}{F} \right) \tag{8}$$

$$\Delta p_{mom} = \frac{G_2^2}{g\rho_1} \frac{\beta + \alpha}{1 - \alpha} \tag{9}$$

and:

$$\Delta p_{vc} = K_c \frac{G_2^2}{2g\rho_1} \tag{10}$$

where K_c is a function of free-flow factor F for the stack, the
value of which was obtained from reference 1. The measured average
half friction factor, also used herein, is similarly defined as:

$$\left(\frac{f}{2} \right)_{meas} = \frac{\Delta p_{meas}}{8 \, \frac{L}{D_e} \, \frac{G^2}{2g\rho_{av}}} \tag{11}$$

PROCEDURE

As previously noted, two stacks of flat plates were used in this
investigation. The plates were spaced 1/4 inch apart in each stack with
either a 1/32-, 1/8-, or 1/4-inch gap between stacks. The two stacks of
plates were first alined in the direction of air flow, and data were ob-
tained at various Reynolds numbers. The average stack temperature level
reported herein was that which resulted from limiting the highest local
temperatures (trailing edge of outside plates) to a safe operating value
for the iron-constantan thermocouples used. Data were similarly ob-
tained for two degrees of plate misalinement, which were obtained by mov-
ing the upstream stack vertically. For the case of slight misalinement,
the upstream stack was moved a distance equal to one plate thickness
(top of plate in upstream stack level with bottom of plate in downstream
stack); while for complete misalinement, the upstream stack was moved
by one-half the distance between plates.

RESULTS AND DISCUSSION

Plate Temperature Gradients

Typical plate temperature gradients obtained for the downstream
stack are presented in figure 5, where local surface temperature $T_{s,l}$
is plotted against distance from plate leading edge X.

The plates are numbered from top to bottom of the stack, but are
listed in an order of symmetry starting from the center plate and moving
toward the outer top and bottom plates. The curves for the three cen-
termost plates are essentially coincident, while the next two plates on
either side of the three centermost plates show slightly higher tempera-
tures at the trailing edges. The curves for the two outside plates fall
considerably above the other curves, particularly at the trailing edge;
this would be expected inasmuch as the top and bottom plates are cooled
on one side only (see fig. 2(a)). The dashed lines, for the four outer-
most plates, represent an approximation of the temperature gradient,
since thermocouples were located only at the leading and trailing edges
of these plates. The average plate and stack temperatures were obtained
from these curves as indicated in the section METHOD OF CALCULATION.

Heat-Transfer Data

Average heat-transfer coefficients for stack.- - The average heat-
transfer coefficients obtained for the downstream stack are presented
in figure 6 where the Nusselt-Prandtl number relation $Nu_b/Pr_b^{0.4}$ is
plotted against Reynolds number D_eG/μ_b. Included for comparison is

the McAdams line (solid) which was found to best represent the data of various investigators (ref. 1) for fully developed turbulent flow in smooth tubes; the equation is:

$$\frac{Nu_b}{Pr_b^{0.4}} = 0.023 \left(\frac{D_e G}{\mu_b}\right)^{0.8} \tag{12}$$

The predicted line (dashed) in figure 6 includes a correction to the conventional McAdams equation (eq. (12)) to account for the increase in average heat-transfer coefficient to be expected with passages of short L/D_e (7.6). This correction was made in reference 2 by inclusion of a power function of L/D_e in equation (12), the equation being:

$$\frac{Nu_b}{Pr_b^{0.4}} = 0.034 \left(\frac{D_e G}{\mu_b}\right)^{0.8} \left(\frac{L}{D_e}\right)^{-0.1} \tag{13}$$

which, for $L/D_e = 60$, becomes equation (12) and, for $L/D_e = 7.6$, becomes

$$\frac{Nu_b}{Pr_b^{0.4}} = 0.028 \left(\frac{D_e G}{\mu_b}\right)^{0.8} \tag{14}$$

represented by the dashed line in figure 6. The magnitude of this increase in the heat-transfer coefficient is further verified in reference 3 (investigation of average and local heat-transfer coefficients as functions of Re and X/D_e for smooth entrance flow through tubes and between parallel flat plates) for the case of uniform heat flux with uniform initial temperature and velocity distributions.

The average heat-transfer coefficients for the downstream stack (fig. 6) are shown for the case of stacks (plates) alined in the direction of air flow with various gap spacings (1/32, 1/8, and 1/4 in.) between stacks, as well as with the upstream stack removed from the tunnel. The data for all configurations are in reasonably good agreement (about 15 percent high) with the predicted line. The effect of gap spacing and removal of the upstream stack is seen to be negligible.

The effect of plate misalinement is shown in figure 7. With the two stacks completely misalined as described in PROCEDURE, the top insulator plate of the upstream stack (see fig. 2(a)) partly blocks off the top passage of the downstream stack. Hence, in order to compare the data for various degrees of misalinement, the average heat-transfer coefficients for the three center plates of the downstream stack were

used in each case. The results are shown in figure 7, with the same co-
ordinates as in figure 6. The data for the alined condition fall
slightly higher than in figure 6 inasmuch as the electrical heat input
was used in evaluating Q for the three center plates. These data are
compared (fig. 7) with those for the completely misalined and slightly
misalined conditions for the various gap spacings investigated. The
effect of plate misalinement also appears to be negligible.

Visual observation of the plates during testing indicated that the
center seven plates of the heated stack remained flat and perfectly
alined with the first stack; the two outside plates, which were cooled
on one side only, showed slight bending.

Local heat-transfer coefficients for center plate. - The local
heat-transfer coefficients obtained for the center plate of the down-
stream stack are presented in figures 8 to 11.

In figure 8, h_l is plotted against X for the case of plates
alined with various gap spacings between stacks, as well as with the
upstream stack removed; this comparison is shown for two values of
Reynolds number. As seen in figure 8, gap spacing and removal of the
upstream stack have no appreciable effect on the local coefficients,
as was also shown for the average coefficients in figure 6.

As explained in METHOD OF CALCULATION, the local heat-transfer co-
efficients were calculated with the assumption of no heat conduction
along the plate. The effect of heat conduction can be taken into ac-
count by use of the following equation (all terms are for the center
plate):

$$\left(\frac{Q'}{S}\right)_l = \left(\frac{Q}{S}\right)_l + bk_m \frac{d^2 T_{s,l}}{dX^2} \tag{15}$$

where the first term (right side, eq. (15)) is defined in equation (2),
and the second term accounts for heat conduction along the plate. The
corrected values of h_l can then be computed; the uncorrected values
of h_l obtained at the highest Reynolds number with the upstream stack
removed from the tunnel are compared with the corresponding corrected
values of h_l in figure 9. The effect of conduction along the plate
is seen to be small; hence, the effect of conduction is neglected in
subsequent discussion.

A comparison of the local heat-transfer coefficients obtained with
the upstream stack removed, and the predicted values of reference 3 is
shown in figure 10 as a variation of local Nusselt number Nu_l with

X/D_e. The values obtained from reference 3 (dashed lines) are for the case of a gas (Pr = 0.73) flowing between parallel flat plates with the conditions of uniform heat flux, constant properties, and uniform temperature and velocity distribution at the entrance. The predicted curves are shown for essentially the same values of inlet Reynolds number Re_i and heat-flux parameter as obtained in the present investigation. At the lowest Reynolds number, the experimental values (solid lines) are in good agreement with those predicted, although slightly higher near the leading edge. With increase in Reynolds number, however, the experimental values are somewhat higher throughout as also indicated by the average coefficients (downstream stack only) in figure 6.

The effect of plate misalinement on the variation of local heat-transfer coefficient along the plate is shown in figure 11 where h_l/h_{av} is plotted against X. The data are shown for the cases of plates alined, slightly misalined, and completely misalined at a Reynolds number of about 40,000 and a 1/8-inch gap between stacks. Figure 11 indicates that plate misalinement results in slightly higher values of h_l/h_{av} at the leading edge and slightly lower values at the trailing edge. The average heat-transfer coefficient for the center plate was essentially the same for all degrees of misalinement, as was also shown in figure 7 for the three center plates.

Friction Data

Average friction factors for upstream stack. - The average half-friction factors obtained for the upstream stack are presented in figure 12 wherein half-friction factor $f/2$ is plotted against Reynolds number $D_e G/\mu_b$. Included, for comparison, is the Kármán-Nikuradse line (solid), representing the relation between friction factor and Reynolds number for turbulent flow in smooth pipes, which is

$$\frac{1}{\sqrt{8\ f/2}} = 2\ \log\left(Re\ \sqrt{8\ f/2}\right) - 0.8 \tag{16}$$

In comparing the data presented herein with those for fully developed turbulent flow (reference line), the effect of L/D_e must be taken into account; this effect consists of (1) a momentum loss in the stack associated with transition from a flat velocity profile at the entrance to some degree of fully developed turbulent velocity profile at the exit, and (2) an increase in average friction factor associated with short L/D_e wherein the entrance effect (region of high local shear stress and friction) may exist over a considerable portion of the passage length. These effects are accounted for in the analysis of reference 3 which predicts friction factors for flow between parallel flat

plates with uniform velocity distribution at the entrance as a function of X/D_e and Reynolds number. Reference 3 indicates that the ratio of average friction factor for X/D_e = 7.6 to the friction factor for fully developed turbulent flow is about 1.54 for the range of Reynolds numbers investigated herein. The predicted line (dashed, fig. 12) represents the reference line (solid) corrected by this ratio.

Two different values of friction factor are presented in figure 12 for the present data: (1) friction factor based on measured static-pressure drop, and (2) friction factor based on measured pressure drop fully corrected for entrance, exit, momentum, and vena contracta losses as explained in the section METHOD OF CALCULATION. The measured values of $f/2$ fall slightly above the predicted line. When the various losses are taken into account, the data fall within ±8 percent of the predicted line.

Average friction factors for downstream stack. - The average half-friction factors for the downstream stack are presented in figure 13 in the same manner as that used for the upstream stack in figure 12. The friction data presented are for a 1/8-inch gap between stacks. The friction factors based on measured pressure drops fall near the predicted line; but when the various losses and the same L/D_e correction used for the upstream stack is taken into account, the data for the downstream stack fall considerably below the predicted line. The L/D_e correction, as previously indicated, is for the case of uniform velocity distribution at the stack entrance. This condition is satisfied for the upstream stack (fig. 12), but it is questionable as to whether the 1/8-inch gap between stacks is adequate to completely flatten out (before it enters the downstream stack) what is essentially a fully developed velocity distribution at the exit of the upstream stack (indicated by ref. 3). The results of figure 13 (overcorrection of the data) indicate that complete flattening out does not occur.

Average friction factors for both stacks combined. - It might be of interest to compare the results in figure 13 with those for the case where no flattening out of the flow at the entrance to the downstream stack is assumed to occur, that is, where the two stacks are considered as a continuous passage. The data for the latter case are presented in figure 14, where the fully corrected friction factors are based on measured pressure drops across both stacks corrected for entrance, exit, momentum, and vena contracta losses, and with the reference line corrected for an L/D_e = 15.2 (dashed line). Friction factors based on measured pressure drops are again included. The fully corrected half-friction factors now fall slightly above the predicted line (data undercorrected). Hence, a comparison of figures 13 and 14 indicates that the velocity distribution at the entrance of the downstream stack is neither uniform nor substantially fully developed as at the exit of the upstream stack.

SUMMARY OF RESULTS

The results of tests to obtain heat-transfer and pressure-drop data for flow of air between electrically heated parallel flat plates, with various gap spacings and degrees of misalinement between stacks, can be summarized as follows:

1. Average heat-transfer coefficients obtained for the downstream stack fell considerably above the conventional McAdams line representing average coefficients for fully developed turbulent flow in smooth tubes of length-diameter ratio L/D_e approximately equal to 60. When the McAdams line was corrected to account for L/D_e effects ($L/D_e = 7.6$), the data gave reasonably good agreement with the predicted line (about 15 percent high). The effects of gap spacing and plate misalinement between stacks were found to be negligible.

2. Local heat-transfer coefficients obtained for the center plate of the downstream stack (with upstream stack removed) were compared with those predicted by analytical methods for flow of a gas (Pr = 0.73) between parallel flat plates for the case of uniform heat flux and initial temperature distribution, and uniform velocity distribution at the entrance. The experimental and predicted values were in fairly good agreement at the lowest Reynolds number, the experimental values becoming somewhat higher with increase in Reynolds number.

3. Average half-friction factors for the upstream stack, when fully corrected for entrance, exit, momentum, and vena contracta losses were in good agreement with a predicted line; which was based on the Kármán-Nikuradse line representing average friction factors for fully developed turbulent flow in smooth pipes with suitable correction for L/D_e effects. The data fell within ±8 percent of the reference line.

4. Average half-friction factors for the downstream stack fell below the predicted line when a uniform velocity profile at entrance was assumed and above the predicted line when a fully developed velocity profile at the entrance was assumed.

Lewis Flight Propulsion Laboratory
    National Advisory Committee for Aeronautics
        Cleveland, Ohio, June 14, 1954

APPENDIX A

SYMBOLS

The following symbols are used in this report:

A   free-flow area, sq ft

b   plate thickness, ft

C   constant

c_p specific heat of air at constant pressure, Btu/(lb)(^{O}F)

D_e effective diameter of stack passage, 4A/Z, ft

E   potential difference, volts

F   free-flow factor (free flow area/total frontal area)

$(f/2)_{meas}$ average half-friction factor based on measured static-
            pressure drop

$(f/2)_{corr}$ average half-friction factor based on measured static-
            pressure drop corrected for entrance, exit, momentum, and
            vena-contracta losses

G   mass velocity (mass flow per unit cross-sectional free-flow
            area) W/A, lb/(hr)(sq ft)

g   acceleration due to gravity, 4.17×10^8 ft/hr^2

h   heat-transfer coefficient, Btu/(hr)(sq ft)(^{O}F)

K_c vena contracta pressure-loss coefficient

k   thermal conductivity of air, Btu/(hr)(sq ft)(^{O}F/ft)

k_m thermal conductivity of plate material,
            Btu/(hr)(sq ft)(^{O}F/ft)

L   length of stack passage, ft

P   power generation, watts

p   static pressure, lb/sq ft abs

Δp_{meas} measured static-pressure drop across stack, lb/sq ft

Δp_{corr} measured static-pressure drop across stack corrected for
                 entrance, exit, momentum, and vena-contracta losses

Δp_{en} entrance pressure drop, lb/sq ft

Δp_{ex} exit pressure drop, lb/sq ft

Δp_{mom} momentum pressure drop, lb/sq ft

Δp_{vc} vena contracta pressure drop, lb/sq ft

Q rate of heat transfer to air, Btu/hr

Q' rate of heat transfer to air (corrected for heat conduction
                 along plate), Btu/hr

R gas constant for air, ft-lb/(lb)($^{\circ}$F)

R' electrical resistance, ohms

r electrical resistivity, ohm-cm

S heat-transfer surface area, sq ft

T air total temperature, $^{\circ}$R

T_b air bulk temperature, $^{\circ}$R

T_s surface temperature, $^{\circ}$R

t static temperature, $^{\circ}$R

Δt static-temperature difference between entrance and exit of
                 stack, $^{\circ}$R

W air flow, lb/hr

X distance from plate leading edge, in.

Z wetted perimeter of stack passage, ft

α $\Delta p_{meas}/p_1$

β $\Delta t/t_1$

μ absolute viscosity of air, $lb/(hr)(ft)$

ρ density of air, $lb/cu\ ft$

Dimensionless parameters:

Nu   Nusselt number, hD_e/k

Pr   Prandtl number, $c_p\mu/k$

Re   Reynolds number, $D_e G/\mu$

Subscripts:

av   average value

b   physical properties evaluated at bulk temperature

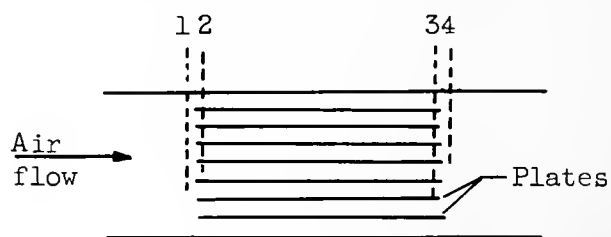i   physical properties evaluated at inlet temperature

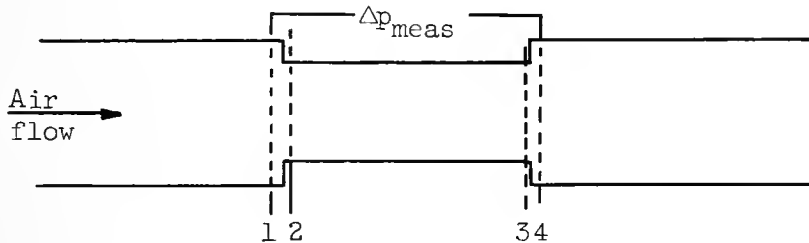l local value

P   plate

st   stack

The following diagrammatic sketch of the stack defines the subscripts
pertaining to various stations:

APPENDIX B

DERIVATION OF PRESSURE LOSS EQUATIONS USED HEREIN

A schematic diagram of the test section (stack) showing the various stations is given below:

Entrance pressure loss Δp_{en}. - A pressure loss occurs in the flow stream in the entrance region between stations 1 and 2. Assuming no friction and fluid incompressibility ($\rho_1 = \rho_2$), the general energy equation between these stations can be written:

$$p_1 + \frac{\rho_1 V_1^2}{2g} = p_2 + \frac{\rho_1 V_2^2}{2g} \tag{B1}$$

Also,

$$V_2 = \frac{A_1}{A_2} V_1$$

hence,

$$\Delta p_{en} = p_1 - p_2 = \frac{\rho_1 V_1^2}{2g} \left[\left(\frac{A_1}{A_2} \right)^2 - 1 \right] \tag{B2}$$

Rewriting equation (B2) in terms of the mass velocity G and the free-flow factor F (defined as A_2/A_1) results in:

$$\Delta p_{en} = \frac{G_2^2}{2g\rho_1} (1 - F^2) \tag{B3}$$

Exit pressure drop Δp_{ex}. - The momentum change between stations 3 and 4, where an expansion occurs, can be stated as follows:

$$\frac{W}{g} V_3 + p_3 A_4 = \frac{W}{g} V_4 + p_4 A_4 \tag{B4}$$

Assuming incompressibility, equation (B4) becomes:

$$\Delta p_{ex} = p_3 - p_4 = \frac{\rho_3 V_3^2}{g} \left[\left(\frac{A_3}{A_4} \right)^2 - \frac{A_3}{A_4} \right] \tag{B5}$$

As before, $A_2/A_1 = F$ and $A_3/A_4 = F$; therefore,

$$\Delta p_{ex} = \frac{G_3^2}{g\rho_3} (F^2 - F) \tag{B6}$$

In order to write equation (B6) in terms of entrance conditions at station 1, the following was assumed:

$$\rho_3 = \frac{p_3}{R t_3} = \frac{p_1 - \Delta p}{R(t_1 + \Delta t)} \tag{B7}$$

The Δp used in equation (B7) was approximated by using Δp_{meas} to avoid a trial-and-error solution. The error incurred by this assumption is negligible.

From equation (B7), equation (B6) can now be written:

$$\Delta p_{ex} = \frac{G_1^2}{g\rho_1} \frac{1 + \beta}{1 - \alpha} (1 - 1/F) \tag{B8}$$

where

$$\alpha = \Delta p/p_1 \tag{B9}$$

and

$$\beta = \Delta t/t_1 \tag{B10}$$

Vena-contracta pressure loss Δp_{vc}. - The vena-contracta pressure loss was taken as a factor K_c times the dynamic pressure in the test section as given by

$$\Delta p_{vc} = K_c \frac{G_2{}^2}{2g\rho_1} \tag{B11}$$

where K_c is a function of the free-flow factor of the test section; values of K_c were obtained from reference 1.

Momentum pressure loss Δp_{mom}. - Using the general momentum equation and assuming $\rho_1 = \rho_2$ result in the following equation

$$\Delta p_{mom} = \frac{G_2{}^2}{g}\left(\frac{1}{\rho_3} - \frac{1}{\rho_1}\right) \tag{B12}$$

Rewriting equation (B12) with the aid of equations (B7), (B9), and (B10) gives

$$\Delta p_{mom} = \frac{G_2{}^2}{g\rho_1}\frac{\beta + \alpha}{1 - \alpha}$$

REFERENCES

1. McAdams, William H.: Heat Transmission. Second ed., McGraw-Hill Book Co., Inc., 1942.

2. Humble, Leroy V., Lowdermilk, Warren H., and Desmon, Leland G.: Measurements of Average Heat-Transfer and Friction Coefficients for Subsonic Flow of Air in Smooth Tubes at High Surface and Fluid Temperatures. NACA Rep. 1020, 1951. (Supersedes NACA RM's E7L31, E8L03, E50E23, and E50H23.)

3. Deissler, Robert G.: Analysis of Turbulent Heat Transfer and Flow in the Entrance Regions of Smooth Passages. NACA TN 3016, 1953.

TABLE I. - TABULATED DATA FOR DOWNSTREAM STACK

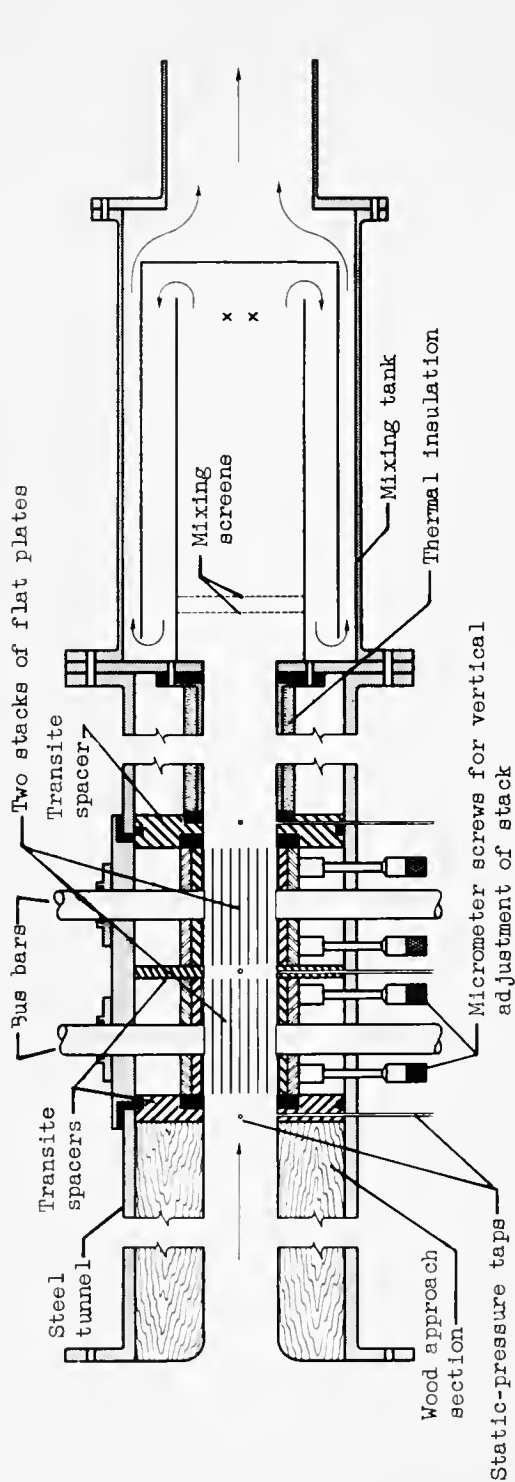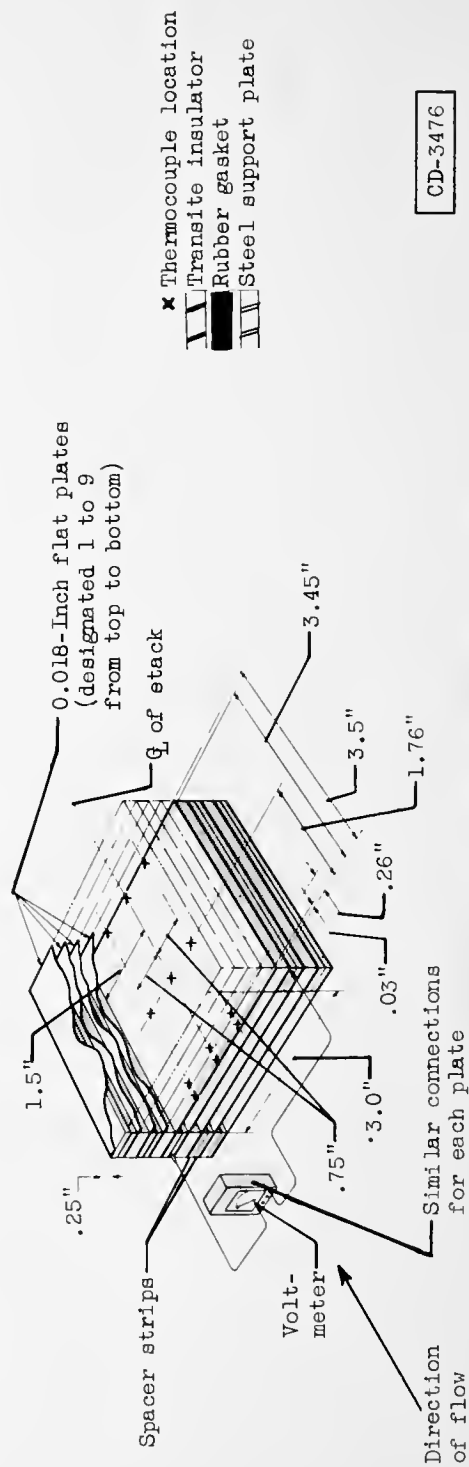| Reynolds number for stack, Re_b	Average surface temperature for stack, $T_{s,av}$, °R	Average air bulk temperature for stack, $T_{b,av}$, °R	Heat-transfer rate for stack, Q, Btu/hr	Heat-transfer rate for plate 5, Q, Btu/hr	Average heat-transfer coefficient for stack, h_{av}, Btu/(hr)(sq ft)(°F)	Temperature rise, $T_4 - T_1$, °F	Air flow, W, lb/hr	Local surface temperature for plate 5, $T_{s,l}$, °F Distance from leading edge of plate, in.				Condition
								0.03	0.26	1.76	3.45	
41,400	665	524	9150	1000	55.6	19.5	1960	94	140	199	222	1/8-inch gap; plates alined
25,800	665	528	5890	652	36.8	20.0	1230	98	140	201	221	1/8-inch gap; plates alined
16,200	672	532	4080	452	25.0	22.0	773	106	141	208	230	1/8-inch gap; plates alined
41,500	669	526	9200	1010	55.1	19.5	1970	95	135	205	225	1/8-inch gap; plates slightly misalined
26,400	667	529	6240	692	38.8	21.0	1240	98	135	208	225	1/8-inch gap; plates slightly misalined
16,400	673	532	4140	453	25.1	22.0	783	102	135	214	229	1/8-inch gap; plates slightly misalined
41,700	666	524	8750	959	52.8	18.5	1970	89	125	190	220	1/8-inch gap; plates completely misalined
26,200	672	528	5970	659	35.5	20.0	1240	94	124	197	225	1/8-inch gap; plates completely misalined
16,300	683	531	3930	434	22.1	21.0	779	100	128	214	240	1/8-inch gap; plates completely misalined
41,400	667	526	9410	1040	57.2	20.0	1960	96	140	198	223	1/32-inch gap; plates alined
26,000	664	527	6200	689	38.8	21.0	1230	100	140	200	225	1/32-inch gap; plates alined
16,200	669	532	4350	484	27.2	23.5	771	107	143	209	233	1/32-inch gap; plates alined
41,500	665	524	9170	1010	55.8	19.5	1960	93	132	201	225	1/32-inch gap; plates slightly misalined
26,100	661	527	6230	691	39.9	21.0	1240	95	131	204	220	1/32-inch gap; plates slightly misalined
16,100	669	531	4140	459	25.7	22.5	766	102	135	218	230	1/32-inch gap; plates slightly misalined
41,700	668	524	8750	963	52.1	18.5	1970	84	123	188	220	1/32-inch gap; plates completely misalined
26,200	662	526	5810	641	36.6	19.5	1241	88	118	188	218	1/32-inch gap; plates completely misalined
16,200	674	530	4080	451	24.3	22.0	772	94	119	202	228	1/32-inch gap; plates completely misalined
41,500	669	526	8970	982	53.7	19.0	1970	94	134	200	224	1/4-inch gap; plates alined
26,100	668	529	6170	684	38.0	20.8	1240	98	135	208	225	1/4-inch gap; plates alined
16,100	675	534	4100	455	24.9	22.0	776	102	136	219	231	1/4-inch gap; plates alined
41,400	668	526	8950	983	54.0	19.0	1960	92	135	200	223	1/4-inch gap; plates slightly misalined
26,000	669	529	6150	682	37.6	20.8	1240	98	135	206	225	1/4-inch gap; plates slightly misalined
16,300	674	532	4090	449	24.7	22.0	775	101	135	215	229	1/4-inch gap; plates slightly misalined
41,400	665	526	8700	954	53.6	18.5	1960	89	125	187	218	1/4-inch gap; plates completely misalined
25,900	666	529	5830	643	36.5	19.8	1230	94	124	193	222	1/4-inch gap; plates completely misalined
16,100	668	532	4050	443	25.5	22.0	766	98	125	208	230	1/4-inch gap; plates completely misalined
41,600	670	524	9430	1040	55.4	20.0	1970	95	134	198	226	First stack removed from tunnel
26,100	673	527	6250	696	36.7	21.0	1240	100	132	210	230	First stack removed from tunnel
16,400	681	532	4230	468	24.3	22.5	783	106	133	233	254	First stack removed from tunnel
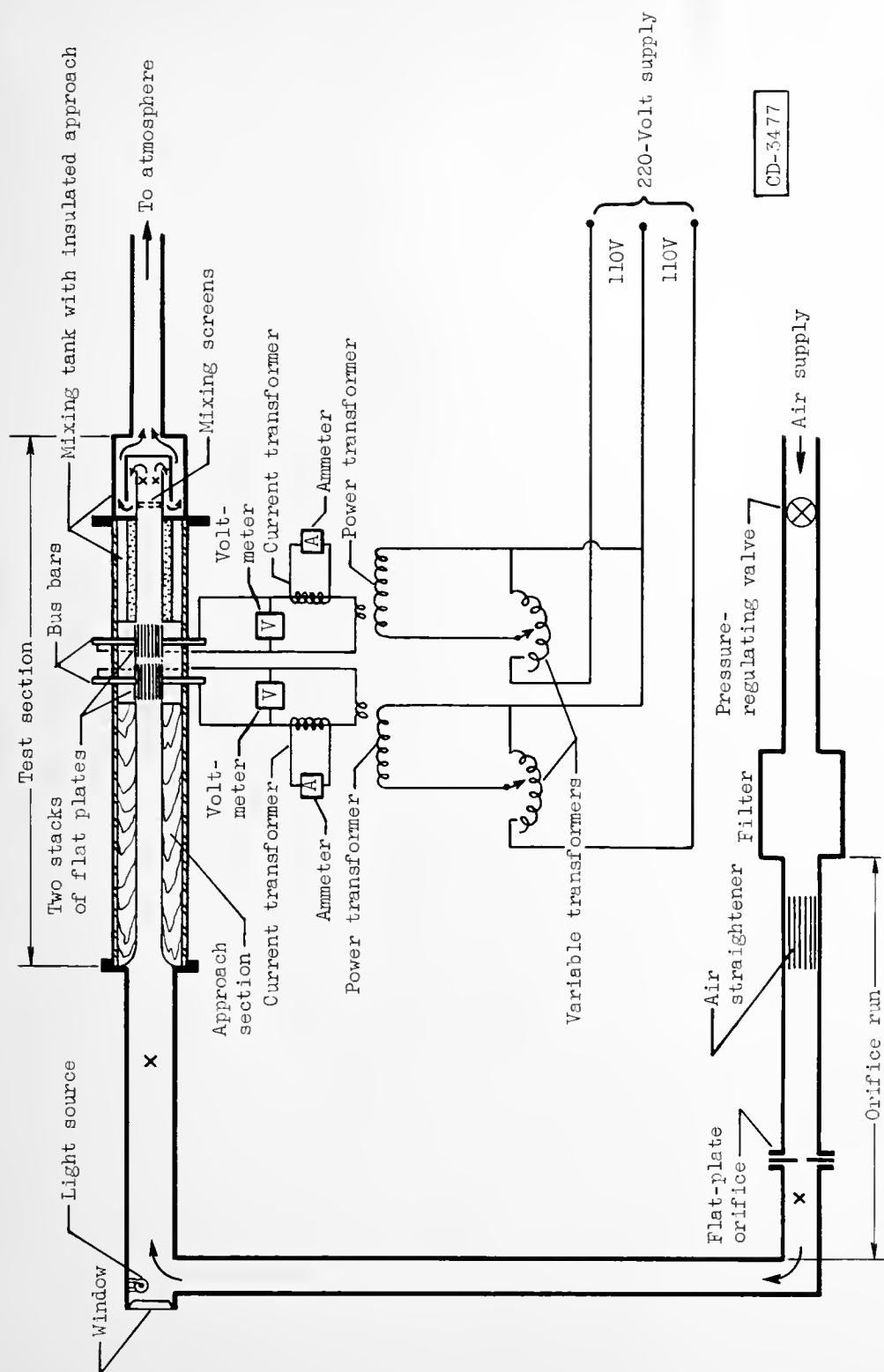
* Thermocouples

Figure 1. - Schematic diagram of test section and related components of air and electrical system.

(a) General view.

(b) Stack of plates showing assembly and instrumentation details.

Figure 2. - Schematic diagram of test section.

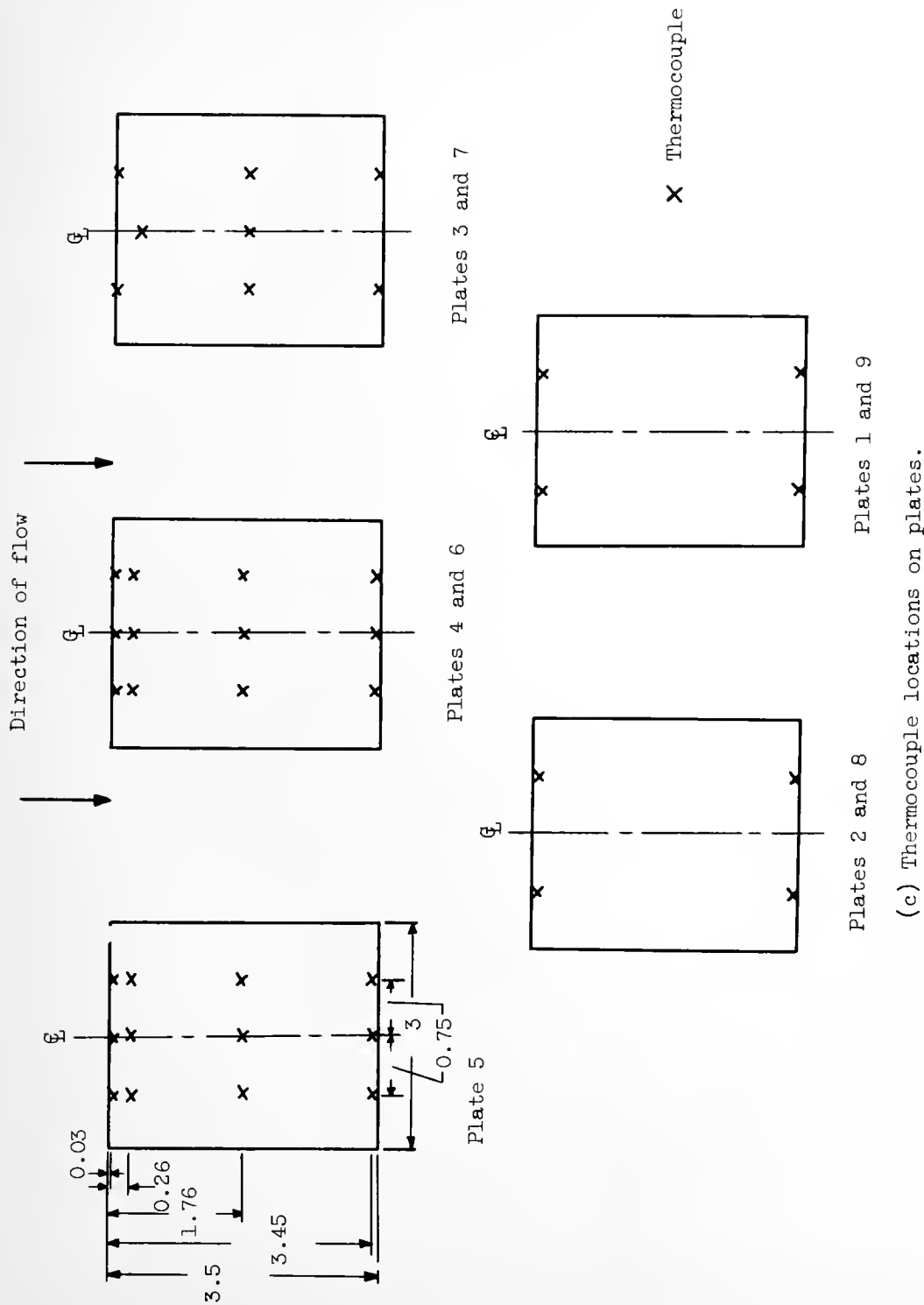(c) Thermocouple locations on plates.

Figure 2. - Concluded. Schematic diagram of test section.
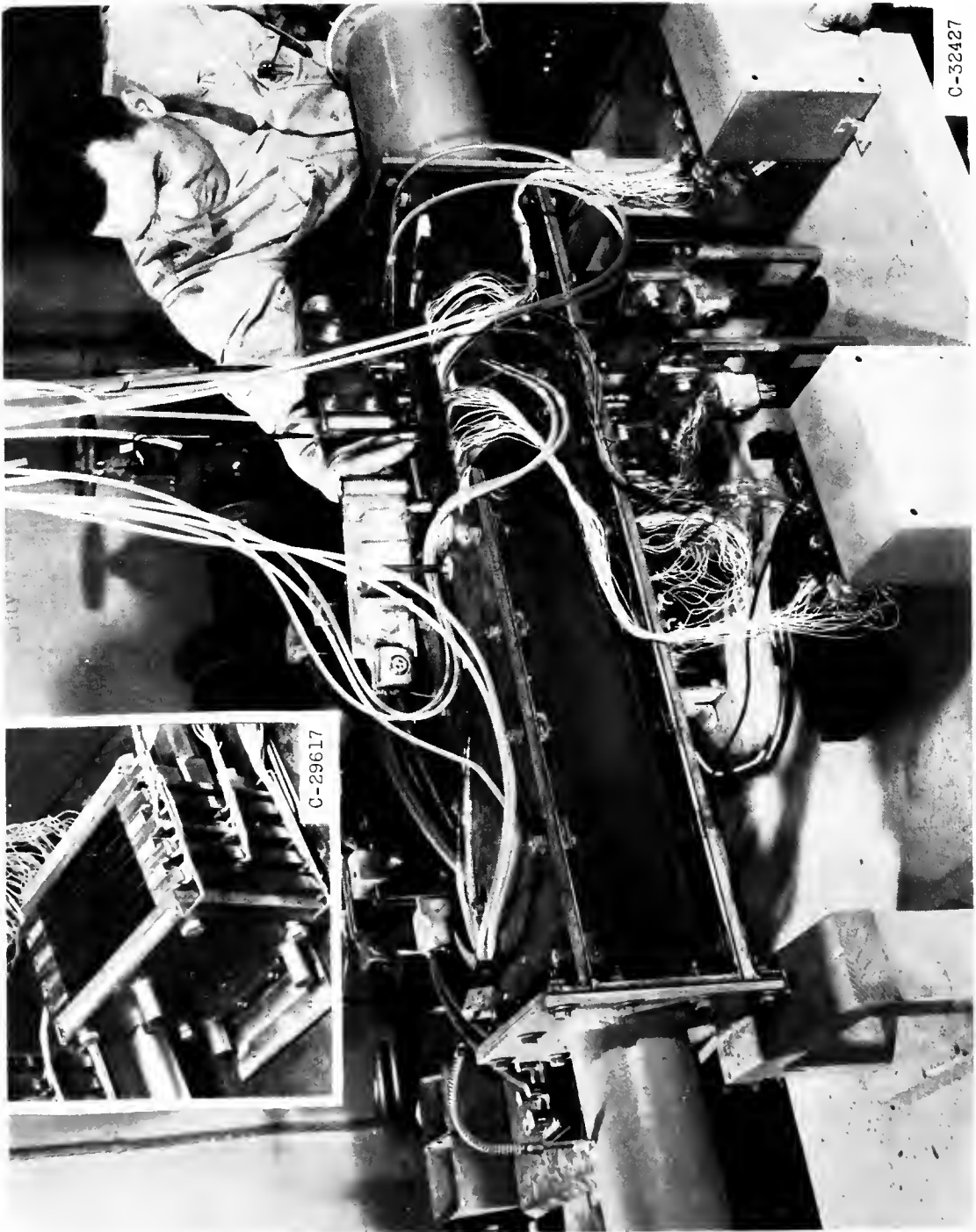
Figure 3. - Photograph of test setup and typical stack assembly (insert).
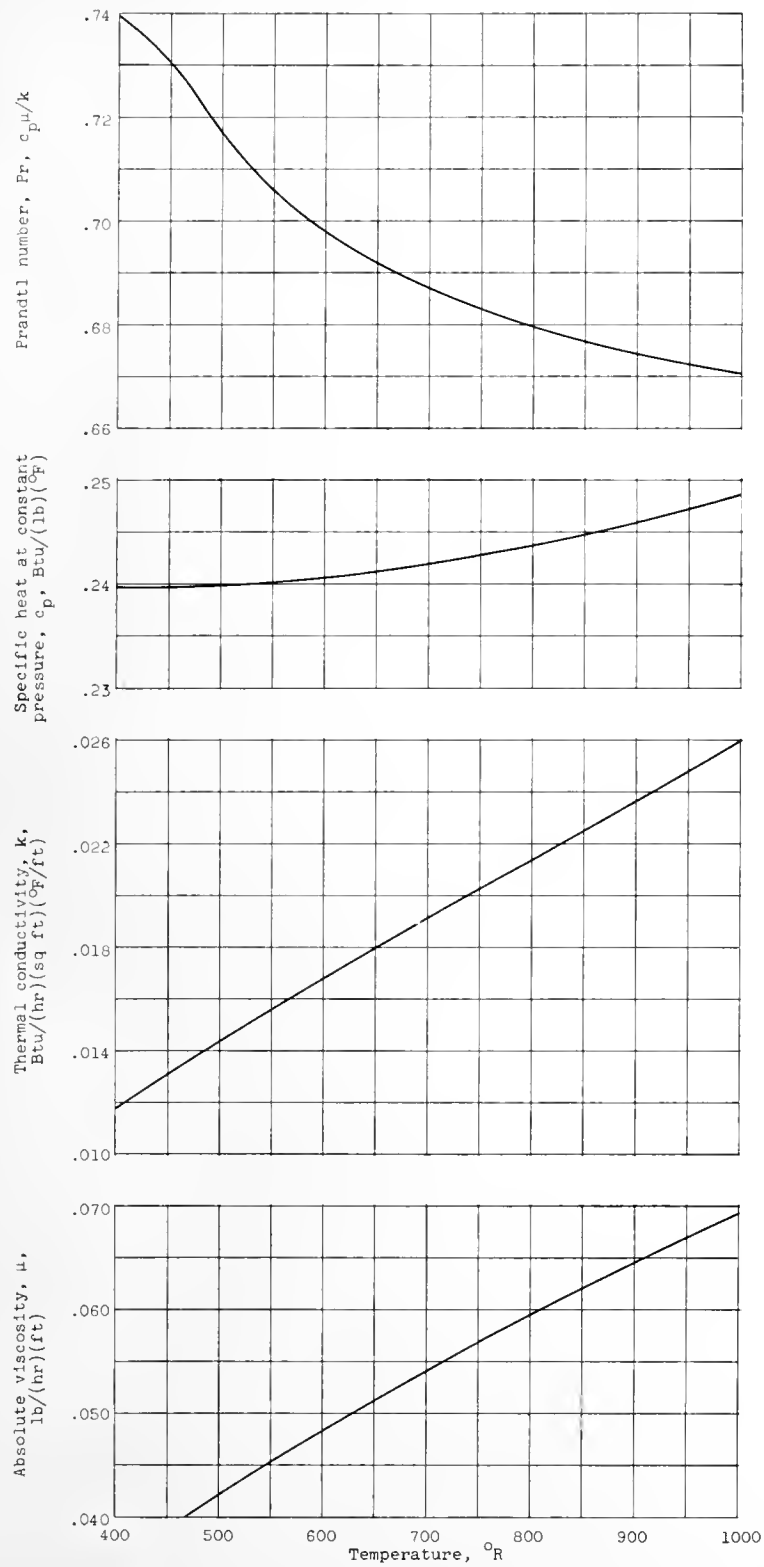
Figure 4. - Physical properties of air over temperature range
400° to 1000° R.

Figure 5. - Typical temperature gradient curves for plates in downstream stack. Average surface temperature for stack, $T_{s,av}$, 665° R; air bulk temperature, T_b, 528° R; heat-transfer rate to air, Q, 5890 Btu per hour; Reynolds number, Re, 25,800; stacks alined.
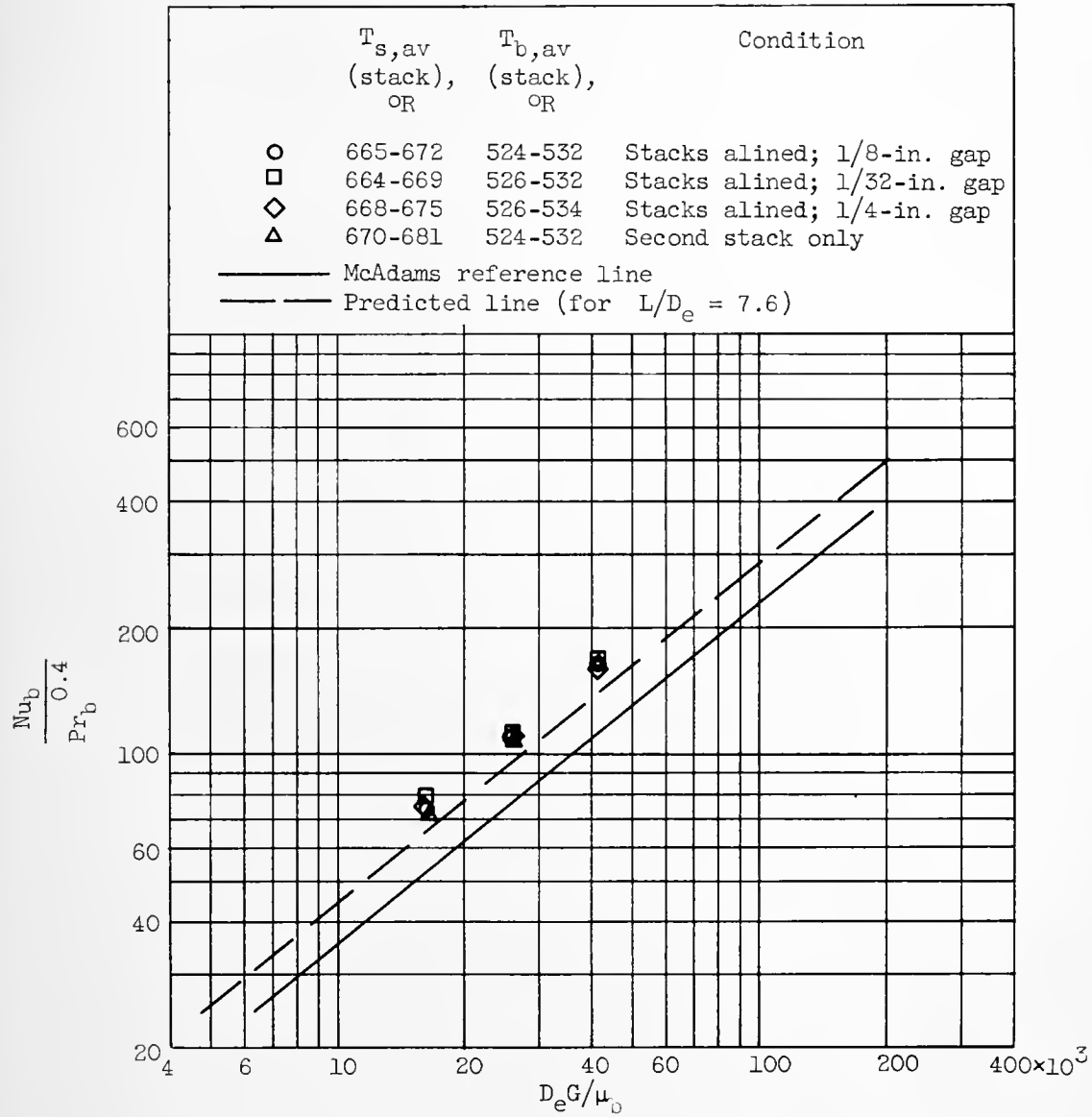
Figure 6. - Average heat-transfer coefficients for downstream
stack as affected by gap between stacks.

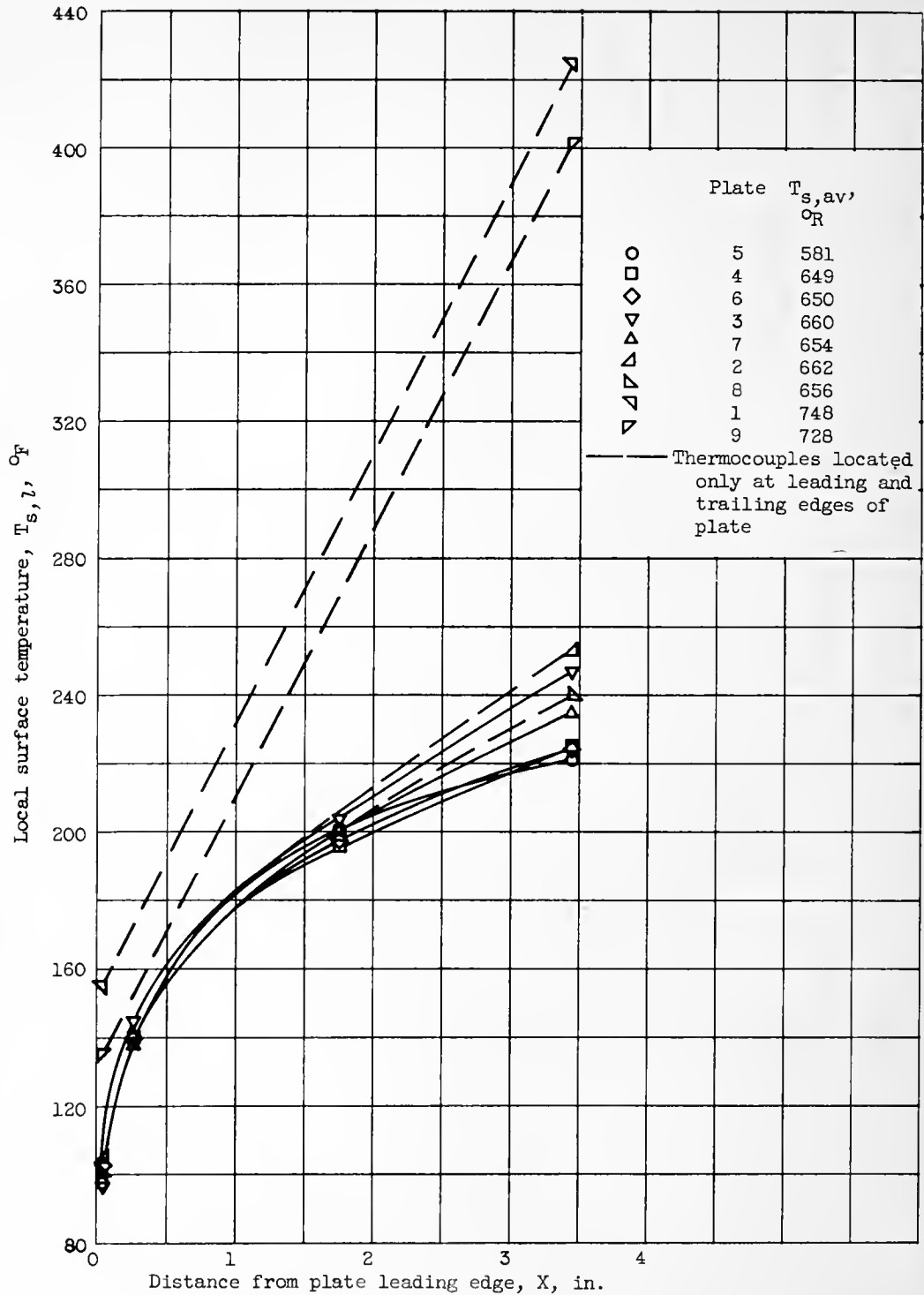|	$T_{s,av}$ (stack), $^\circ R$	$T_{b,av}$ (stack), $^\circ R$	Condition	Gap spacing, in.
O	665-672	524-532	Alined	1/8
◖	667-673	526-532	Slightly misalined	1/8
◗	666-683	525-531	Completely misalined	1/8
□	664-669	526-532	Alined	1/32
◪	661-669	524-531	Slightly misalined	1/32
◩	662-674	524-530	Completely misalined	1/32
◇	668-675	526-534	Alined	1/4
◈	668-674	526-532	Slightly misalined	1/4
◈	665-668	526-532	Completely misalined	1/4
——	Predicted line (for L/D_e = 7.6)			

Figure 7. - Average heat-transfer coefficients for three center plates of downstream stack as affected by plate misalinement and gap between stacks.

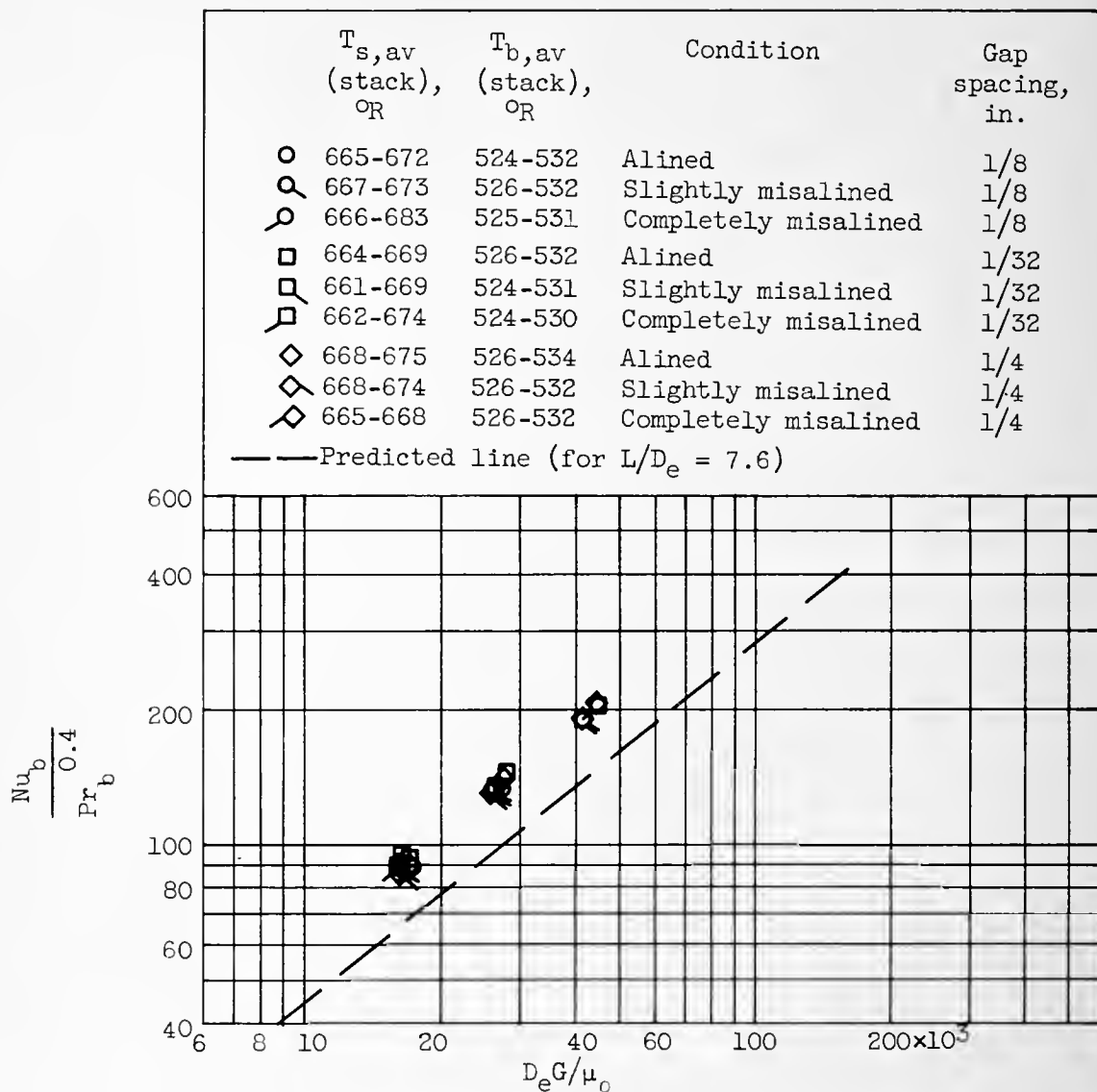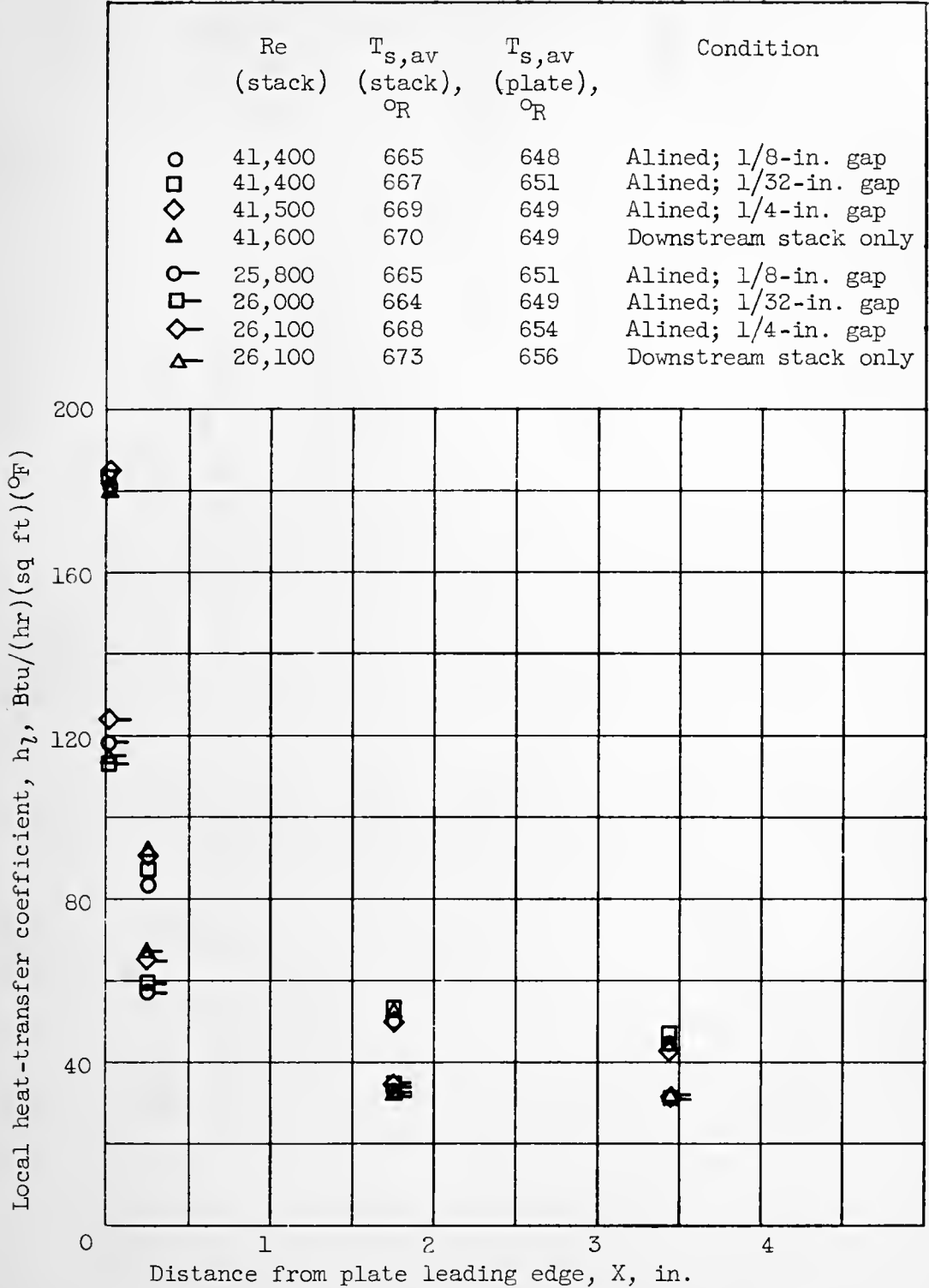|	Re (stack)	$T_{s,av}$ (stack), $^{\circ}R$	$T_{s,av}$ (plate), $^{\circ}R$	Condition
○	41,400	665	648	Alined; 1/8-in. gap
□	41,400	667	651	Alined; 1/32-in. gap
◇	41,500	669	649	Alined; 1/4-in. gap
△	41,600	670	649	Downstream stack only
○—	25,800	665	651	Alined; 1/8-in. gap
□—	26,000	664	649	Alined; 1/32-in. gap
◇—	26,100	668	654	Alined; 1/4-in. gap
△—	26,100	673	656	Downstream stack only

Figure 8. - Local heat-transfer coefficients for center plate of downstream stack as affected by gap between stacks.
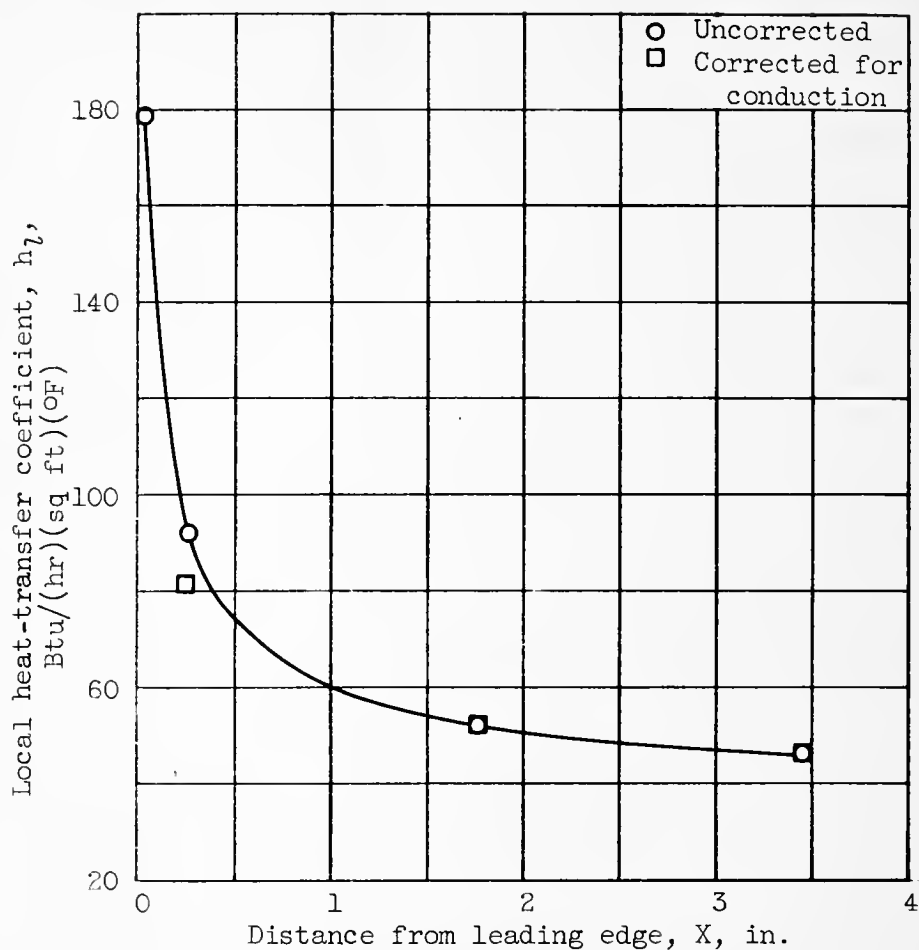
Figure 9. - Local heat-transfer coefficients for
center plate of downstream stack, with upstream
stack removed from tunnel, as affected by heat
conduction along plate. Average surface temper-
ature, $T_{s,av}$; for stack, 670° R; for plate 5,
649° R; average bulk temperature for stack,
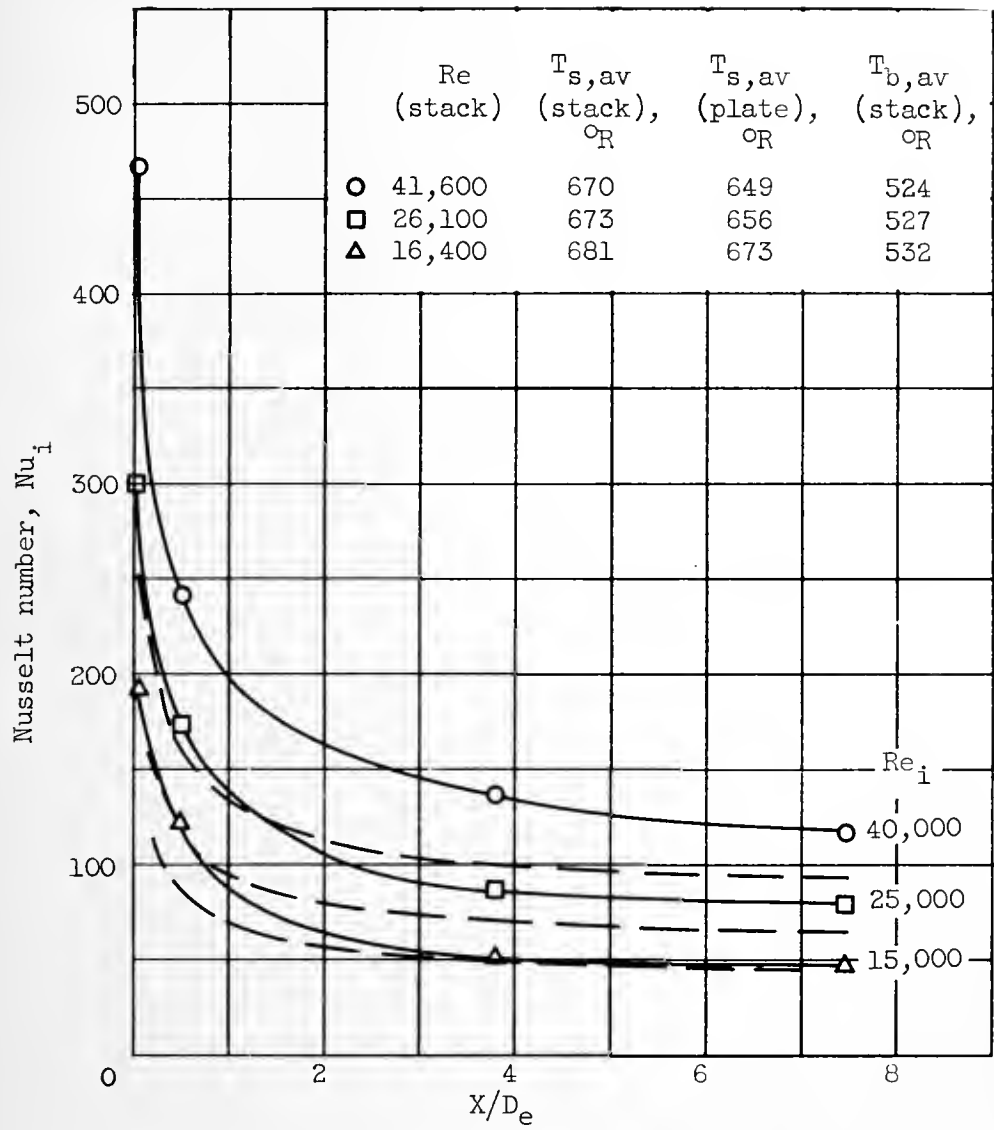524° R; Reynolds number, Re, 41,600.

Figure 10. - Local values of Nusselt number for center
plate of downstream stack, with upstream stack removed,
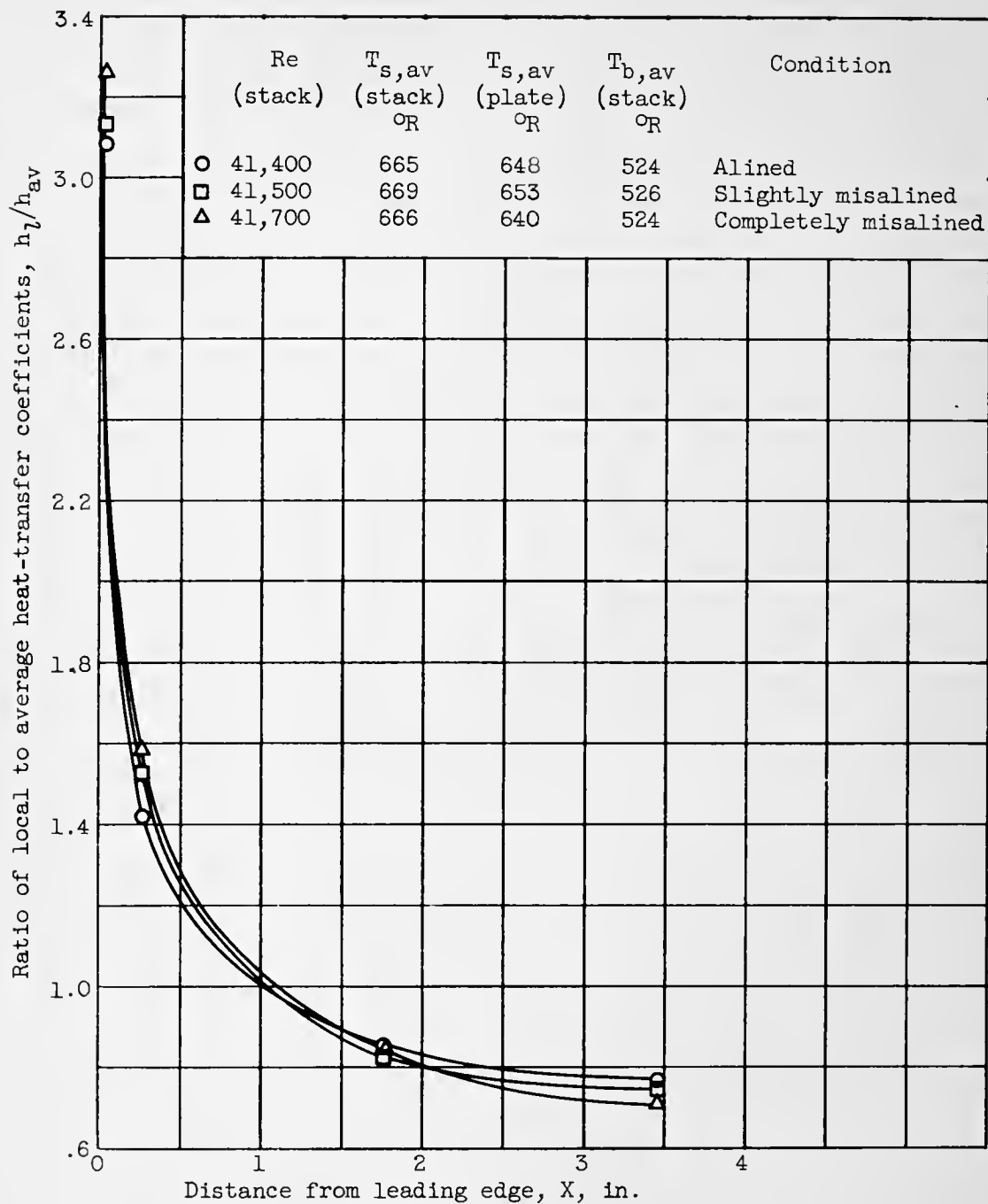as compared with predicted curves of reference 3.

Figure 11. - Ratio of local to average heat-transfer coefficients for center plate of downstream stack for various degrees of plate mis-alinement and 1/8-inch gap between stacks.
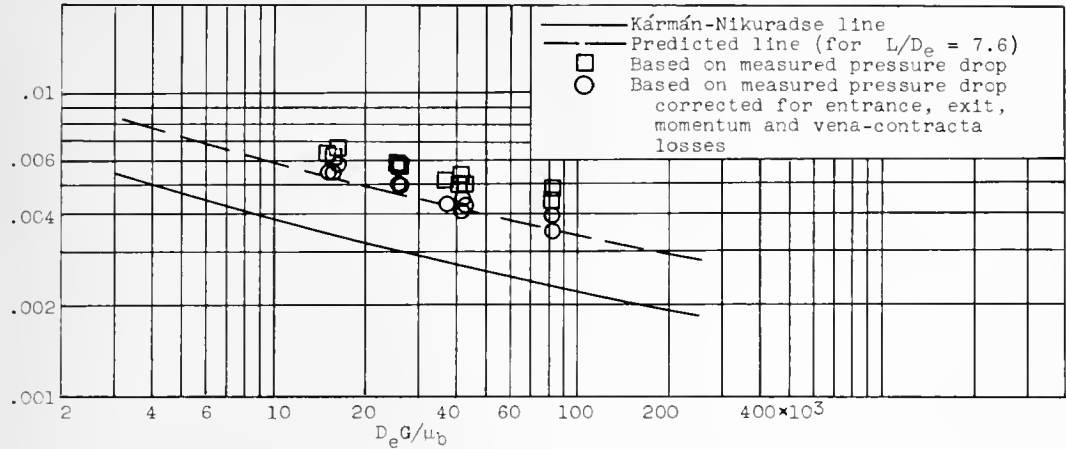
Figure 12. - Average half-friction factors for upstream stack, based on measured values of static-pressure drop, and measured pressure drops corrected for entrance, exit, momentum, and vena-contracta losses.
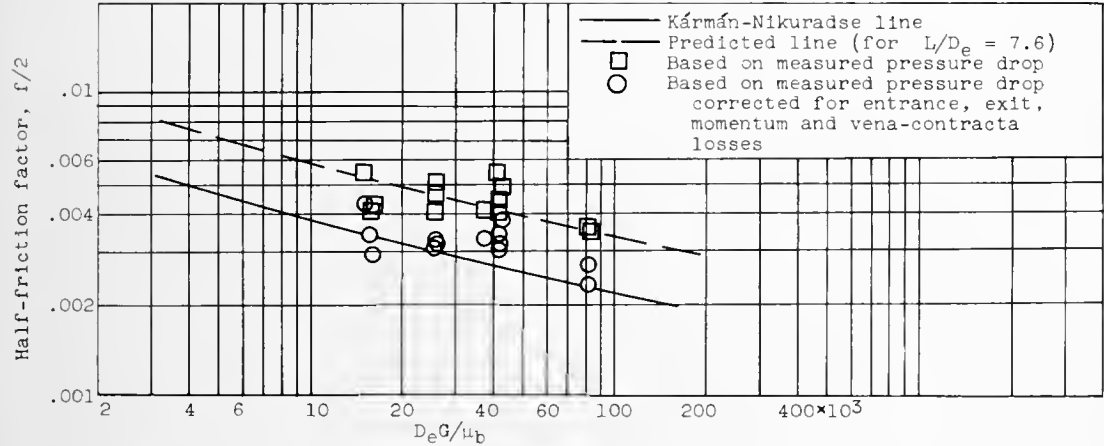
Figure 13. - Average half-friction factors for downstream stack, based on measured values of static pressure drop, and measured pressure drops corrected for entrance, exit, momentum, and vena-contracta losses.

Figure 14. - Average half-friction factor for upstream and downstream stacks combined, based on measured values of static-pressure drop, and measured pressure drops corrected for entrance, exit, momentum, and vena-contracta losses.
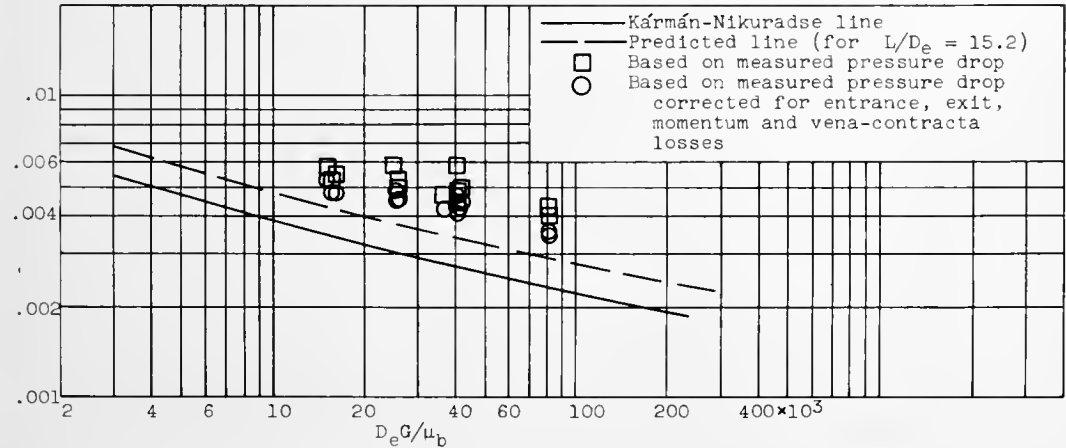
NACA RM E54F11
National Advisory Committee for Aeronautics.
EXPERIMENTAL HEAT-TRANSFER AND FRICTION
COEFFICIENTS FOR AIR FLOWING THROUGH
STACKS OF PARALLEL FLAT PLATES. Eldon W.
Sams and Walter F. Weiland, Jr. August 1954. 33p.
diagrs., photo., tab. (NACA RM E54F11)

Forced-convection heat-transfer and pressure-drop
data were obtained for stacks of parallel flat plates of
short length-to-effective-diameter ratio. Two such
stacks were alined and misalined in the direction of
air flow with gap spacings between stacks of 1/32,
1/8, and 1/4 inch. Data were obtained with heat addi-
tion to the downstream stack only over a range of
Reynolds number from 15,000 to 80,000 and average
surface temperatures of about 680° R. The average
and local heat-transfer coefficients were only slightly
higher than predicted values from established round
tube data. The friction data for both stacks are com-
pared.

Copies obtainable from NACA, Washington

1. Heat, Additions of -
   Aerodynamic (1.1.4.3)
2. Heat Transfer, Theory
   and Experiment (3.9.1)
I. Sams, Eldon W.
II. Weiland, Walter F., Jr.
III. NACA RM E54F11

NACA

NACA RM E54F11
National Advisory Committee for Aeronautics.
EXPERIMENTAL HEAT-TRANSFER AND FRICTION
COEFFICIENTS FOR AIR FLOWING THROUGH
STACKS OF PARALLEL FLAT PLATES. Eldon W.
Sams and Walter F. Weiland, Jr. August 1954. 33p.
diagrs., photo., tab. (NACA RM E54F11)

Forced-convection heat-transfer and pressure-drop
data were obtained for stacks of parallel flat plates of
short length-to-effective-diameter ratio. Two such
stacks were alined and misalined in the direction of
air flow with gap spacings between stacks of 1/32,
1/8, and 1/4 inch. Data were obtained with heat addi-
tion to the downstream stack only over a range of
Reynolds number from 15,000 to 80,000 and average
surface temperatures of about 680° R. The average
and local heat-transfer coefficients were only slightly
higher than predicted values from established round
tube data. The friction data for both stacks are com-
pared.

Copies obtainable from NACA, Washington

1. Heat, Additions of -
   Aerodynamic (1.1.4.3)
2. Heat Transfer, Theory
   and Experiment (3.9.1)
I. Sams, Eldon W.
II. Weiland, Walter F., Jr.
III. NACA RM E54F11

NACA

NACA RM E54F11
National Advisory Committee for Aeronautics.
EXPERIMENTAL HEAT-TRANSFER AND FRICTION
COEFFICIENTS FOR AIR FLOWING THROUGH
STACKS OF PARALLEL FLAT PLATES. Eldon W.
Sams and Walter F. Weiland, Jr. August 1954. 33p.
diagrs., photo., tab. (NACA RM E54F11)

Forced-convection heat-transfer and pressure-drop
data were obtained for stacks of parallel flat plates of
short length-to-effective-diameter ratio. Two such
stacks were alined and misalined in the direction of
air flow with gap spacings between stacks of 1/32,
1/8, and 1/4 inch. Data were obtained with heat addi-
tion to the downstream stack only over a range of
Reynolds number from 15,000 to 80,000 and average
surface temperatures of about 680° R. The average
and local heat-transfer coefficients were only slightly
higher than predicted values from established round
tube data. The friction data for both stacks are com-
pared.

Copies obtainable from NACA, Washington

1. Heat, Additions of -
   Aerodynamic (1.1.4.3)
2. Heat Transfer, Theory
   and Experiment (3.9.1)
I. Sams, Eldon W.
II. Weiland, Walter F., Jr.
III. NACA RM E54F11

NACA

NACA RM E54F11
National Advisory Committee for Aeronautics.
EXPERIMENTAL HEAT-TRANSFER AND FRICTION
COEFFICIENTS FOR AIR FLOWING THROUGH
STACKS OF PARALLEL FLAT PLATES. Eldon W.
Sams and Walter F. Weiland, Jr. August 1954. 33p.
diagrs., photo., tab. (NACA RM E54F11)

Forced-convection heat-transfer and pressure-drop
data were obtained for stacks of parallel flat plates of
short length-to-effective-diameter ratio. Two such
stacks were alined and misalined in the direction of
air flow with gap spacings between stacks of 1/32,
1/8, and 1/4 inch. Data were obtained with heat addi-
tion to the downstream stack only over a range of
Reynolds number from 15,000 to 80,000 and average
surface temperatures of about 680° R. The average
and local heat-transfer coefficients were only slightly
higher than predicted values from established round
tube data. The friction data for both stacks are com-
pared.

Copies obtainable from NACA, Washington

1. Heat, Additions of -
   Aerodynamic (1.1.4.3)
2. Heat Transfer, Theory
   and Experiment (3.9.1)
I. Sams, Eldon W.
II. Weiland, Walter F., Jr.
III. NACA RM E54F11

NACA